International Journal of Fluid Dynamics (2002) **Vol 7**, Article 1, 1–7
Available online at: http://elecpress.monash.edu.au/ijfd

Thermal and Hydrodynamic Visualisation of a Water Jet Impinging on a Flat Surface using Microencapsulated Liquid Crystals

S. Ashforth-Frost[1] & U.W. Rüdel[2]
[1] *School of Engineering, The Nottingham Trent University, Burton Street, Nottingham, NG1 4BU, UK.*
[2] *ALSTOM Power Technology Centre, Cambridge Road, Whetstone, Leicester, LH8 6LH, UK.*

Keywords: Impinging jet(s), Liquid crystals, Velocity fields, Temperature field

(Received Publication date October 12 2003.)

Thermochromic liquid crystals have been extensively applied to natural convection flows for the visualisation of temperature and induced velocity fields. In this study, results of the simultaneous visualisation of velocity and temperature in a forced convection flow are presented. The single submerged impinging water jet was artificially seeded with microencapsulated liquid crystals. A nozzle to plate spacing of three nozzle diameters and a turbulent Reynolds number of 35500 was considered. Visualisation of the flow field revealed the thermal development of the impinging and resultant wall jet as well as the high temperature gradients that prevail at the impingement surface. In particular, entrainment of heated spent fluid at the nozzle exit and in the shear layer region was observed. Flow characteristics typical of turbulent impinging jets were visualised; vortices, initiated at the edge of the jet are transported to the stagnation region, a wall jet develops which rolls back and changes direction. The observed hysteresis in calibration curves for heating and cooling of the liquid crystals was quantified. The use of liquid crystals as particle tracers has been demonstrated as a useful tool for the simultaneous quantitative visualisation of flow and temperature in a forced convection flow.

1. INTRODUCTION

Impinging jets are widely used in heating and cooling applications due to their excellent heat transfer characteristics. To optimise heat transfer an understanding of the temperature field as well as the velocity field is essential, in particular near the impingement surface where the flow characteristics dominate the heat transfer process. Heat transfer distributions of jet impingement and the effect of various geometric and flow parameters on heat transfer are well documented, for example by Jambunathan et al. (1992) and Viskanta (1993). Gas jets and liquid jets have been investigated. The link between near wall velocity and turbulence and their effect on heat transfer has been known for a long time Gardon and Akfirat (1965) but Cooper et al. (1993) were among the first to provide much needed velocity measurements using hot-wire anemometry. Ball et al. (1998) obtained detailed velocity and temperature near wall data for a cold air jet impinging on to a hot surface using hot and cold-wire anemometry. However, there still remains a paucity of information describing the temperature field of impinging jets.

The development of liquid crystal techniques for temperature measurement, coupled with image and data processing, has opened some new avenues for heat transfer and fluid flow research. Thermochromic liquid crystals illuminated by white light reflect different colours, at specific wavelengths, in response to a change in their temperature. The colour change is reversible and the attainable accuracy is comparable to, or better than, conventional thermocoupling. Their rate of response has been shown to be of the order of a few milliseconds by Ireland and Jones (1987). Liquid crystal formulations can be manufactured to suit a particular experiment so that they exhibit the visible spectrum over small (0.5° C) or large (30° C) temperature ranges within an overall range of -20° C to 120° C . Their use as indicators for surface temperature measurements is well established and they have been applied to a wide range of engineering situations world wide, in particular in heat transfer testing. Less exploited is the use of liquid crystals, as artificial seeding particles suspended in a fluid, to determine flow temperatures. There is some archived literature that renders the technique promising. In the 1980's, results were usually recorded using conventional photography and white light illumination. Several ways of interpreting colour based on hue, saturation or intensity (HSI) information, are discussed by Dabiri and Gharib (1991). Initially, narrow band filters were used to identify a single colour, or a range of filters used to identify several. However, since the early 1990's colour image processing has been employed, which can yield full field temperature information from a single image, to within $< 0.1°$ C. Liquid crystals as seeding particles for quantitative temperature measurements have been widely exploited. Recently, the technique has been extended to the visualisation of three-dimensional temperature fields, Lutjen et al. (2001). The use of liquid crystals for simultaneous quantitative velocity and temperature measurements, has been less exploited; see for example, Ashforth-Frost et al. (1996), Ozawa et al. (1992) and Braun et al. (1993). Typically, velocities have been derived using a cross-correlation technique whilst (from the same images) temperatures were quantified by a temperature versus hue relationship. These previous works have been confined to natural convection with the exception of a limited amount of work involving mixed convection, Prasad and Koseff (1996).

This paper demonstrates the potential of using microencapsulated thermochromic liquid crystals, for the simultaneous visualisation of flow and heat transfer in a forced convection flow namely, an impinging water jet. A jet to plate spacing of 3 diameters was investigated at an average Reynolds number of 35500.

2. EXPERIMENTAL PROCEDURE

For full field flow visualisation purposes, liquid crystals have, in the past, proved difficult to apply to forced convection flows due to their becoming easily mechanically damaged during circulation through the experimental rig, see for example Ashforth-Frost and Jambunathan (1993). This has been overcome using a steady gravity fed fluid supply from a reservoir (maintained at an elevated temperature), which was recirculated using a peristaltic pump, see Figure 1. Jet Reynolds number was maintained at $35500 \pm 2\%$. The fluid used was de-ionised and filtered water, which was artificially seeded with 0.08% (by volume) thermochromic microencapsulated liquid crystals (Hallcrest BM/R29C4W/S33). At the start of the test, water at 34° C was allowed to flow from the nozzle (developing velocity profile) into the impingement region which was contained within a 0.15 m × 0.15 m × 0.1 m tank. The impingement plate and surrounding fluid were initially at 27° C. Temperatures in the reservoir and in the tank were monitored by means of conventional K-type thermocouples. A thin sheet of white light, from a cold light source (1000W Quartz Tungsten Halogen lamp), was used to illuminate the flow. The flow field was viewed at right angles to the light. Images of the liquid crystals were recorded using a CCD-camera (25 frames per second, 752 × 582 picture elements). A FlashBus MV Plus PCI frame grabber digitised the analogue signal into 24 bits-per-pixel colour images, see Keating et al. (1998).

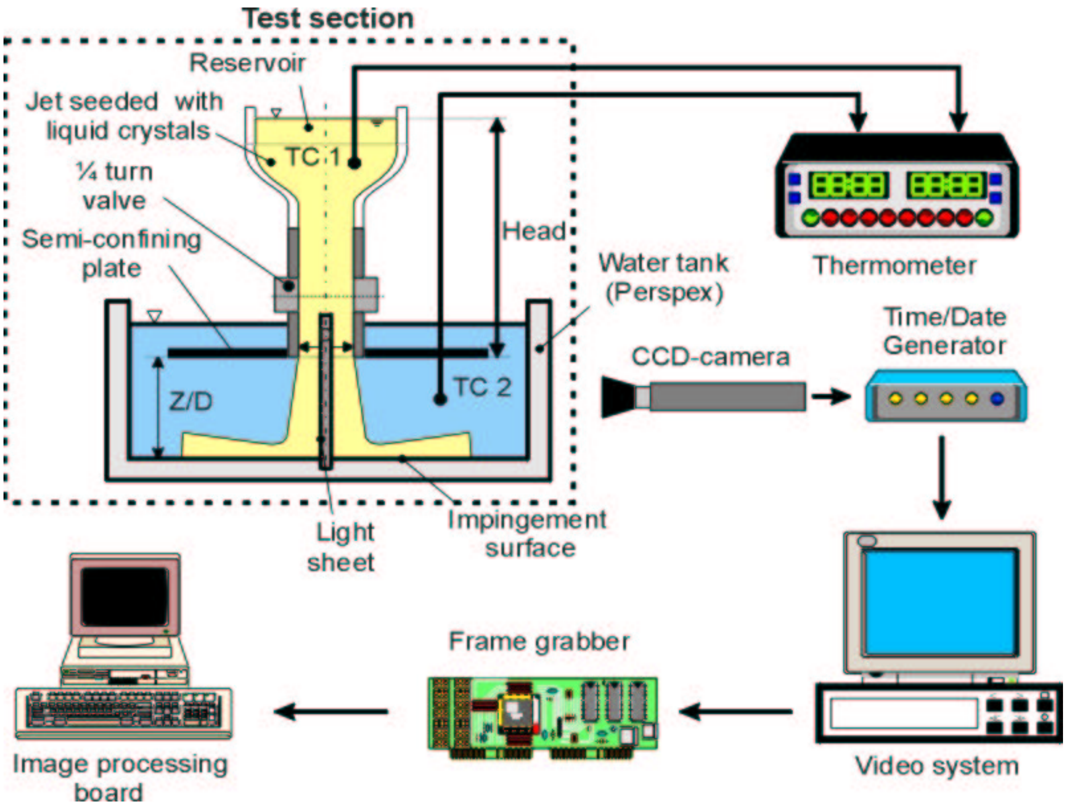

Figure 1. Schematic of the experimental rig and data collection and processing.

Calibration of the liquid crystals (HSI) was achieved by immersing a vessel, containing the artificially seeded water, in a water bath maintained at constant temperatures. Illumination, viewing and recording arrangements used were the same as those used in the experimental tests described above. Temperatures were monitored by an immersed K-type thermocouple, connected to a multi-meter (Keithley digital 2001) incorporating a scanner card. In an earlier study (Ashforth-Frost and Jambunathan, 1993) it was observed that, on cooling, liquid crystal seeding particles, exhibiting different colours, exist at the same time. Consequently, calibration was performed during heating and cooling of the test fluid.

This was at a thermal gradient of 0.75° C/min., which represented the average temperature change over the test duration.

3. RESULTS AND DISCUSSION

Accuracies better than $< 0.1°$ C are often achieved using liquid crystals in heat transfer testing when the liquid crystal coated surface is heated. However, despite being generally considered as a fully reversible process, the hue versus temperature calibration revealed a hysteresis effect between heating and cooling of approximately 0.25° C; the higher temperatures being associated with the cooling process. This was anticipated and is an inherent characteristic of the liquid crystals. A possible explanation is that on heating, the liquid crystals pass from their cholesteric (crystalline) phase, during which they exhibit brilliant colours, to an isotropic phase (colourless). The hysteresis effect is attributed to mal-alignment of the crystals during cooling (isotropic to cholesteric phase transition) which leads to a reduction in brightness and change in calibration. This alignment is dependent on the rate of cooling. Consequently, these effects will become significant where rapid heating and cooling occurs, in the same flow domain, where the liquid crystals are allowed to pass from crystalline to isotropic state and back.

A series of still images of the flow is shown in Figure 2 and moving images in Figure 3. Initially, vortices are initiated at the exit of the round jet, due to prevailing high shear levels, and are transported downstream towards the stagnation region. The potential core and the deflection of the jet at the impingement surface can be observed. Wall eddies are formed which accelerate along the plate stretching and diverging in the radial direction. Downstream, the deflected flow develops into a wall jet. A larger scale recirculation forms (confined by the parallel impingement and nozzle plates) and the resultant wall jet rolls back with direction reversal, defining a separation point. The separation point moves downstream as the test progresses. Entrainment of low temperature fluid occurs between the recirculation and the nozzle plate. The spread of the jet and position of the recirculation region compares favourably with that described by Saripalli (1983) for a similar geometry and turbulent Reynolds number.

The most interesting aspect of the images is the thermal visualisation. Initially, the liquid crystals are suddenly exposed to a high temperature gradient. The fast response of the liquid crystals would allow even the early stages of the impinging jet to be observed. However, the rapid colour change cannot be captured such that they appear to act as any seeding particle, reflecting white light, as they would when above or below their temperature range. As they cool down they enter the colour/temperature range for which they were prepared (cholesteric phase) and exhibit colours.Initially the hot jet impinges on the cold impingement surface in the tank. In the potential core of the jet the exhibited temperature is in the red-orange-yellow range. This is a consequence of the ongoing mixing process between the hot jet fluid and the cold tank fluid. It should be noted that, at this stage of the test, the overall local temperature in this region (interface jet/stagnant fluid) is dominated by the temperature of the fluid in the tank. This is due to the fact that the water in the tank represents a reservoir due to its greater fluid quantity and, therefore, its greater thermal inertia; the liquid crystals in the issuing hot jet are cooled down by the cold fluid in the tank. This process is helped and augmented by the very high thermal conductivity of water. As the test progresses the local temperature in this region becomes dominated by the jet temperature. The temporal

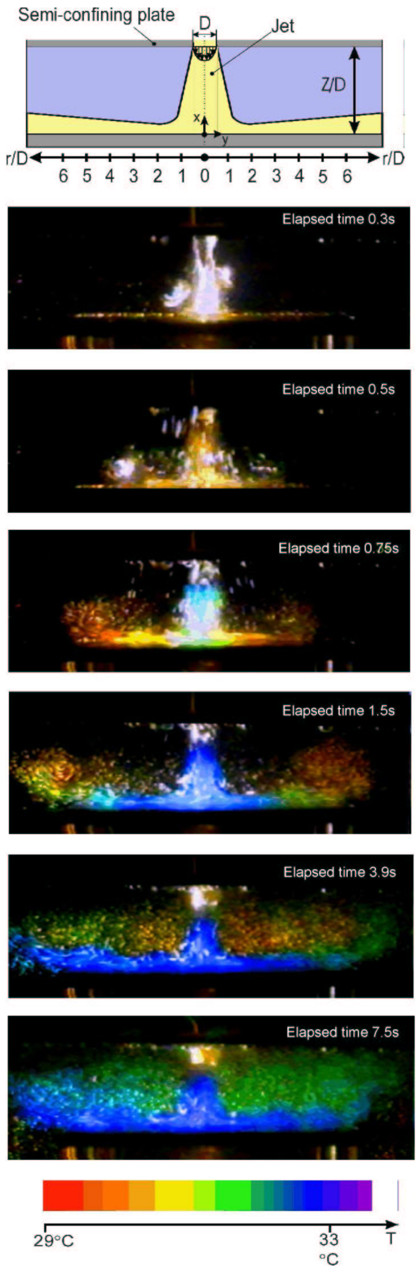

Figure 2. Still images of the flow at different time showing thermal field.

thermal development of the wall jet is clearly visible, the thermal boundary layer becoming thicker as temperature gradients fall. The temperature of the wall jet decays fastest where

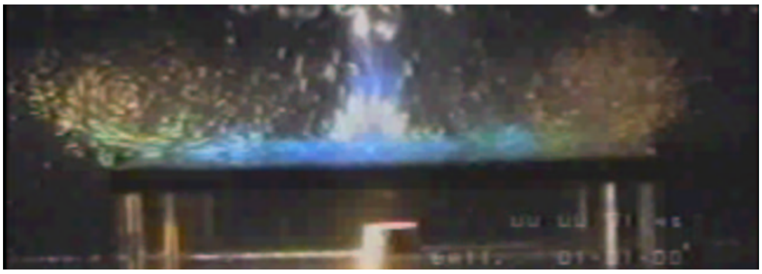

Figure 3. Still image from animation of flow and thermal fields (see website).

high heat transfer prevails, namely, in the stagnation region. At the edge of the wall jet, pockets of fluid with high rotational energy break away and are transported back towards the impinging jet. This leads to entrainment of already spent fluid (i.e. already heated) back into the impinging jet. This is evident from the colour change in the potential core region of the jet; initially the hot jet is cooled to the lower end of its colour change temperature. As the test progresses the jet increases in temperature (from red, through the full colour spectrum, to blue). Eventually, the space between the parallel plates becomes heated due to this entrainment of spent fluid. The flow is complex and the boundary layer appears as wavy streamlines between the vortices and the impingement plate.

4. CONCLUDING REMARKS

Visualisation of the temperature field revealed the thermal development of the impinging and resultant wall jet and, in particular, entrainment of spent fluid at the nozzle exit and in the shear layer region. A velocity field typical of impinging jets has been described. Despite hysteresis effects observed in the calibration of thermochromic liquid crystals, they have been demonstrated as a useful tool for gaining a simultaneous insight into the hydrodynamic and thermal flow features of a turbulent impinging jet. It is suggested that these hysteresis effects may be reduced by not allowing the liquid crystals to progress from their crystalline state to their isotropic state; the tests should be performed with maximum and minimum temperatures which correspond to the temperature range for which the liquid crystal formulation was prepared (that is to say, within the colour spectrum). In-situ calibration (at a point in the tank) where the fluid temperature is recorded alongside the colour isotherms, although intrusive, would allow further assessment of the thermal accuracy and add confidence to the technique.

Acknowledgements

Appreciation is expressed to the Engineering and Physical Science Research Council (Grant AF/97/0568 to the first author).

References

1. Earnshaw, P.B. and Lawford, J.A. (1966) Low-Speed Wind Tunnel Experiments on a Series of Sharp-Edged Delta Wings, ARC R&M No. 3424. Abdulmouti, H., Murai, Y., Ohno, Y. and Yamamoto, F. (2001) Measurement of Bubble Plume Generated Surface Flow Using PIV, *Journal of the Visualization Society of Japan*, **21** (2), 31–37.
2. Ashforth-Frost, S., Ju, X.Y., Jambunathan, K. and Wu, X. (1996) Application of liquid crystals to particle image velocimetry. *Proc. IMechE Int. Symp. Optical Methods and Data Processing in Heat and Fluid Flow*, 81–89.
3. Ashforth-Frost, S. and Jambunathan, K. (1993) Flow visualisation using liquid crystals. *Proc. SPIE Int. Symp. Optical Instrumentation and Applied Science: Optical Diagnostics in Fluid and Thermal Flow*, 237–244.
4. Ball, S.J., Ashforth-Frost, S., Jambunathan, K. and Whitney, C.F. (1998) Orthogonally impinging axisymmetric jet investigation; heat transfer and near wall thermal flow field characteristics. *Proc. 11th IHTC*, 5, August 23-28, Kyongju, Korea, 457–462.
5. Braun, M.J., Dzodzo, M. and Lattime, S.B. (1993) Automatic computer based non-intrusive temperature measurements in laminar natural convection using TLC in enclosures with variable aspect ratio. *Experimental and Numerical Flow Visualization*, **172**, 111–119.
6. Cooper, D., Jackson, D.C., Launder, B.E. and Liao, G.X. (1993) Impinging jet studies for turbulence model assessment—I: Flow field experiments. *Int. J. Heat Mass Transfer*, **36**, (10), 2675–2684.
7. Dabiri, D. and Gharib, M. (1991) Digital particle image thermometry: The method and implementation. *Experiments in Fluids*, **11**, 77–86.
8. Ireland, P.T. and Jones, T.V. (1987) The response time of a surface thermometer employing encapsulated thermochromic liquid crystals. *J. Phys. E: Sci. Instrum.*, **20**, 1195–1199.
9. Gardon, R. and Akfirat, J.C. (1965) The role of turbulence in determining the heat transfer characteristics of impinging jets. *Int. J. Heat Mass Transfer*, **8**, 1261–1272.
10. Jambunathan, K., Lai, E., Moss, M.A. and Button, B.L. (1992) A review of heat transfer data for single circular jet impingement. *Int. J. Heat Fluid Flow*, **13**, 106–115.
11. Keating, M.R., Hannis, J.M., Ashforth-Frost, S. and Jambunathan, K. (1998) Heat transfer testing within model gas turbine high pressure rotor blade cooling passages. *Proc. IMC Int. Conf. Mechanics in Design*, 412–422.
12. Lutjen, P.M., Mishra, D. and Prasad. V. (2001) Three-Dimensional Visualization and Measurement of Temperature Field using Liquid Crystal Scanning Thermography. *Trans. ASME*, **23**, (5), 1006–1014.
13. Ozawa, M., Müller, U., Kimura, I. and Takamori, T. (1992) Flow and temperature measurement of natural convection in a Hele-Shaw cell using a thermo-sensitive liquid-crystal tracer. *Experiments in Fluids*, **12**, 213–222.
14. Prasad, A.K. and Koseff, J.R. (1996) Combined forced and natural convection heat transfer in a deep lid-driven cavity flow. *Int. J. Heat Fluid Flow*, **17**, 460–467.
15. Saripalli, K.R. (1983) Visualisation of flow patterns induced by an impinging jet issuing from a circular planform. *AIAA Journal*, **21**, (12), 1764–1766.
16. Viskanta, R. (1993) Heat transfer to impinging isothermal gas and flame jets. *Exp. Thermal Fluid Sci.*, **6**, 111–134.